University of Tehran Press

Online ISSN: 2345-475X

DESERT

Home page: https://jdesert.ut.ac.ir/

Aeolian-Fluvial Interactions in Sandy Sediments of Northeastern Iran: Insights from Quartz Grain Microtextures and Particle Size Distribution

Alireza Karimi[1*], Fatemeh Jafarpour[1]

[1] Department of Soil Science, Faculty of Agriculture, Ferdowsi University of Mashhad, Mashhad, Iran.
Email: karimi-a@um.ac.ir

Article Info.

Article type:
Research Article

Article history:
Received: 28 Mar. 2026
Received in revised from: 25 May 2026
Accepted: 26 May 2026
Published online: 27 May 2026

Keywords:
Aeolian Processes,
Particle size distribution,
Quartz surface microtexture,
Skewness,
Sorting.

ABSTRACT

This study characterized the particle size distribution and surface microtexture of quartz in sandy sediments in southern Sabzevar to identify the nature of these sediments and the processes affecting their accumulation. Thirty samples were collected from 0 to 30 cm at ~1 km intervals along a transect in three geomorphic surfaces: the Kal-e Shur floodplain (FP), the dune field area (DF), and the distal part of the alluvial fan (DA). Particle size analysis revealed bimodal distributions in FP and DA, with modes in fine sand and very coarse silt, indicating mixed aeolian and fluvial sources. In contrast, the DF surface exhibited a unimodal distribution dominated in fine sand, consistent with aeolian processes. Mean grain size (Mz) averaged 4.1 (FP), 3.05 (DF), and 3.61 phi (DA), and sediments were poorly to very poorly sorted across all surfaces. SEM microtextural analysis of quartz grains showed V-shaped percussion marks, conchoidal fractures, and dissolution features. These textures, combined with grain mgorphology (angular to sub-rounded in FP and DA; rounded to sub-rounded in DF), independently support the interpretation of aeolian dominance in the DF and mixed aeolian-fluvial processes in FP and DA. The integration of particle size distribution, quartz microtexture, and geomorphic context effectively discriminates sedimentary processes in this transitional arid landscape.

Cite this article: Karimi, A.R., Jafarpour, F. (2026). Aeolian-Fluvial Interactions in Sandy Sediments of Northeastern Iran: Insights from Quartz Grain Microtextures and Particle Size Distribution. DESERT, 31 (1), DOI: 10.22059/jdesert.2026.107641

DOI: 10.22059/jdesert.2026.107641

Publisher: University of Tehran Press

1. Introduction

Aeolian sediments cover large portions of the world's continents and play a key role in shaping the landscapes (Yang and William, 2015; Tsoar et al., 2009). According to global maps of dryland distribution, roughly 36% of continental land lies under arid or semi-arid climates (Tsoar et al., 2009; Huang et al., 2020). While sandy sediments can be found across all climate zones- from arid to humid-the most extensive deposits occur in desert environments. Their composition and structure can alter in response to physical and chemical processes, including wind, fluvial processes, and climate (Tsoar et al., 2009).

Research on aeolian systems and the geomorphology of arid and semi-arid regions has advanced rapidly in recent years. Significant new studies have focused on aeolian and fluvial sediments, the processes that shape them, and how these processes interact across dryland environments worldwide (Yang and William, 2015; Zhang et al., 2018). Sandy sediments are of particular interest because of their distinctive physical and chemical properties, which researchers examine from multiple aspects. These include mineralogical composition, particle size distribution, sand grain surface textures, pedological characteristics, and sediment provenance (Li et al., 2015; Wang et al., 2017).

Particle size distribution is one of the most useful characteristics of sandy sediments for understanding how they were transported and deposited, and for tracing their provenance (Wang et al., 2003; Abouda, 2003; Zhou et al., 2014; Zhou and Yu, 2014; Zhang and Dong, 2015; Zhang et al., 2015). Wang et al. (2003), for example, found that in the Taklamakan Desert, dunes consist mainly of fine and very fine sand (2–4 phi). The average particle size varies by dune type as 3.08 phi in barchan dunes, 3.21 phi in dome-shaped dunes, 2.81 phi in star dunes, and 2.36 phi in compound sandy dunes. These differences in average particle size, reflect the distinct processes that shape each dune form. Another important line of inquiry involves the morphological characteristics of aeolian sand grains, specifically their shape, roundness, sphericity, and surface texture. These features are important for identifing the modes of transport and deposition (Wass et al., 2014; Ma et al., 2024).

In northeastern Iran, recent studies have focused on characterizing aeolian and playa sediments. Pourali et al. (2023) examined the Sabzevar playa, located in the northeast of the Great Kavir, and found that quartz grain micromorphology differs between aeolian surface sediments and alluvial deep grains. Their findings suggest that the Sabzevar region experienced a shift from warm-humid to warm-arid climates, a transition that has direct implications for understanding modern sediment dynamics in the area. Elsewhere in Iran, Ghazi et al. (2019) used grain size distribution and quartz microtexture analysis to determine the aeolian and fluvial grains within the same sampling transects. Zandifar et al. (2024) documented polymodal sediment sources in Hamoun Hirmand, southeastern Iran, attributing the grain size variations to the combined influence of fluvial and aeolian transport systems.

In Iran, ergs and dunefields cover roughly 2.9% of the country, concentrated in the central and eastern regions. Major ergs include the Yalan Sand Sea in the Lut Desert, as well as the Jen, Shotori, and Kashan-Ardestan ergs surrounding the Great Kavir (Maghsoudi and Ganjaeian, 2025a and b). Recent sedimentological research on barchan dunes in the Erg of Tabas has revealed mean grain sizes ranging from 2.41 to 2.77 phi, with fine sand making up the majority (69.55%). Discriminant analysis further suggests that 87.3% of these sediments are of aeolian origin (Ghayeni et al., 2025).

Although sandy sediments are abundant across Iran's arid and desert regions, relatively little information has been published about them. Khorasan-e Razavi Province, for instance, contains extensive areas of aeolian sediments, yet basic information about their characteristics remains

scarce. One of the important of these depositst lies in the southeastern part of Sabzevar city, covering roughly 165 km² along the edge of the Great Kavir, the largest desert in Iran. The Great Kavir itself is a complex aeolian-fluvial system, where playa sediments, alluvial fans, and dune fields all interact (Pourali et al., 2023). Our study area occupies a critical transition zone, between mountain fluvial systems on one side and desert aeolian processes on the other. The aim of this study was to investigate particle size distribution and quartz grain surface microtextures across three geomorphic surfaces in southern Sabzevar (floodplain, dune field, and distal alluvial fan). In particular, we wanted to see whether these proxies could help distinguish mixed aeolian-fluvial processes in this transitional setting, where both wind and water have shaped sediment accumulation.

2. Materials and Methods

2.1. Study area

The study area is one of the largest aeolian sediment regions south of Sabzevar city. The Sabzevar basin encompasses part of the southern slopes of the Alborz mountain range, extending southwestward toward the Kavir basin. More specifically, our study area locates about 8 kilometers south of Sabzevar city, covering a sandy plain of approximately 165 km². It is situated between latitudes 35° 55' 54" to 36° 10' 10" N and longitudes 57° 46' 38" to 57° 35' 31" E (Figure 1).

The region receives an average annual rainfall of 191.6 mm, with a mean annual temperature of 18.3°C. The prevailing local wind across the Sabzevar plain follows an east–west direction with mean velocity of 18 m/s. According to the De Martonne classification, the area has a hot and dry climate. This aridity, combined with the strength and frequency of the dominant winds, has contributed to the formation of extensive sandy plains throughout the region.

The study area is a small, open basin within a much larger sedimentary corridor extending from Neyshabur to the Great Kavir. Locally, the geology is dominated by the Sabzevar Ophiolite Complex (Upper Cretaceous), which includes peridotites, gabbros, and volcanic rocks such as basalts, andesites, and rhyolites. These rocks formed in a supra-subduction zone setting (Omrani et al., 2018; Shafaii Moghadam et al., 2025). However, the sediment composition has not originated solely from local bedrock. The Kal-e Shur River transports alluvial materials from the distant Neyshabur highlands onto the floodplain (FP). Together, the local ophiolitic highlands and these distal inputs from the Kal-e Shur River serve as the primary sediment sources for this study.

2.2. Sampling and laboratory analyses

Using a combination of geomorphological evidence, Google Earth imagery, field surveys, and visible changes in sediment appearance, we identified three geomorphic surfaces with sandy sediments: the Kal-e Shur river floodplain (FP), the dune field area (DF), and the distal part of the alluvial fan (DA). Each of the three geomorphic surfaces has its distinct topography. The Kal-e Shur floodplain (FP) is almost flat, with a gentle gradient sloping toward the river channel. The dune field (DF) features moderately undulating terrain. The distal alluvial fan (DA), has a subtle yet consistent southeastward slope.

Thirty surface samples (0–30 cm depth) were taken at roughly one‑kilometer intervals along a transect from the floodplain (FP) to the distal alluvial fan (DA). At each point, five subsamples-from the four corners and center of a 20 meter square- were collected and mixed into a single composite sample.

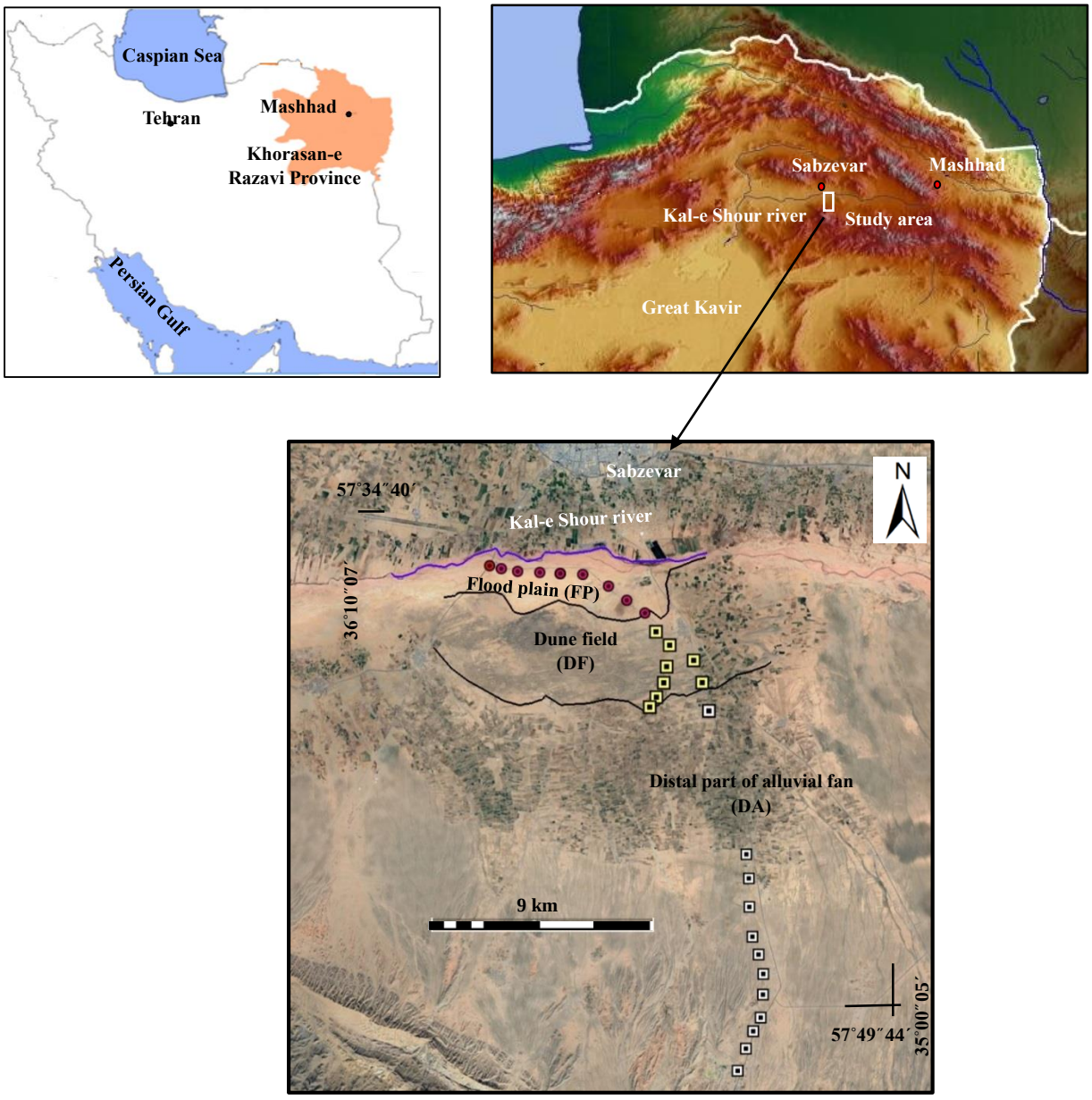

Figure 1. The location of study area, geomorphic surfaces and sampling sites in southern Sabzevar, northeastern Iran

After air-drying, the samples were passed through a 2 mm sieve. For each sample, we used 50 grams to determine particle size distribution. First, the silt and clay fractions (smaller than 63 µm) were separated from the sand fraction. The finer fractions (63-20, 20-5, 5-2, and < 2 µm) were then measured using the pipette method, which relies on differences in settling time within suspension (Burt, 2004). The sand fractions were separated using a series of dry sieves at 0.5 phi intervals in an electric shaker, and the percentages for each interval were calculated.

For micromorphological analysis, we used a scanning electron microscope (SEM). Two samples were collected from each geomorphic surface. Before analysis, calcium carbonate was removed from the sand samples using concentrated hydrochloric acid. The samples were analyzed at Central lab in Ferdowsi University of Mashhad for SEM studies and were examined using a LEO-Germany

VP 1450 microscope. Energy dispersive spectrometer analysis (EDS) analysis was used to ensure that the surface microtexture of quartz grains was examined. At least twenty quartz grains per sample were examined to obtain a representative characterization of their surface textures.

2.3. Data analysis

After weighing each particle fraction and calculating its percentage, we determined the particle size distribution parameters -mean diameter (Mz), sorting (δI), skewness (SKI), and kurtosis (K)- using the GRADISTAT software (Blott and Pye, 2001). These parameters were calculated following the graphical method of Folk and Ward (1957), based on the equations below:

$$Mz = \frac{\varphi 16 + \varphi 50 + \varphi 84}{3}$$

$$\sigma \mathrm{I} = \frac{\varphi 84 - \varphi 16}{4} + \frac{\varphi 95 - \varphi 5}{6.6}$$

$$SKI = \frac{\varphi 16 + \varphi 84 - 2\varphi 50}{2(\varphi 84 - \varphi 16)} + \frac{\varphi 5 + \varphi 95 - 2\varphi 50}{2(\varphi 95 - \varphi 5)}$$

$$K = \frac{\phi 95 - \phi 5}{2.44(\phi 75 - \phi 25)}$$

In the above equations, for example, φ84 represents the diameter of particles in phi scale, where 84% of the particles are smaller than it.

3. Results and discussion

3.1. Particle size distribution

Tables 1 and 2 present the particle size distribution characteristics and a summary of the statistical results for the three geomorphic surfaces of floodplain (FP), dune field (DF), and distal alluvial fan (DA). Sand content varied across the three surfaces. On the FP, it ranged from 20.3% to 73%, with a mean of 42.7%. The DF exhibited higher sand content, ranging from 66.5% to 86.3% (mean 74.1%). On the DA, sand content ranged from 28.3% to 73.2%, averaging 48.1%. The mean sand content across all three surfaces was 54.3%.

Silt content also differed among the surfaces. On the FP, silt content ranged from 23.8% to 76% (mean 54.7%). The DF showed lower silt content, between 12.6% and 30.6% (mean 23.5%), while the DA displayed intermediate values, ranging from 24.6% to 65.8% (mean 48.1%). Clay content exhibited less pronounced variation. It ranged from 0.4% to 5% (mean 2.6%) on the FP, from 1.1% to 3.7% (mean 2.4%) on the DF, and from 1.5% to 6.2% (mean 3.7%) on the DA (Tables 1 and 2).

In the FP surface, fine sand and very coarse silt had the highest frequency with averages of 17.5% and 28.3%, respectively, and in the DA surface with averages of 14.7% and 29.2%. In the DF surface, fine sand was the dominant fraction with an average of 32.9% (Figure 2).

Particle size distribution is a widely used indicator for identifying sediment types and interpreting sedimentary environments (Dong et al., 2011; Zhou et al., 2014; Zhang et al., 2015; Ma et al., 2024). In most sandy sediments, fine and medium sand are the dominant fractions. Zhang et al. (2018), for instance, reported similar findings in the eastern desert regions of China. Comparable patterns have been observed in other arid settings worldwide, including the Toshka region (Hamdan et al., 2015), the Erdos deserts (Rao et al., 2008), the Badain Jaran sand dunes (Dong et al., 2013), and the Ejina desert (Zhou and Yu, 2014). In all of these cases, sediment size typically ranges from fine to medium sand. The geomorphic surfaces examined in our study consist of finer material, ranging from very coarse silt to fine sand.

Table 1. Grain size distribution and statistical parameters of sediments in the geomorphic surfaces

Geomorphic surface	Sample code	Gravel	Sand	Silt	Clay	VCS	CS	MS	FS	VFS	VCSi	CSi	MSi	FSi	VFSi	Mz	□I	SKI	K
		%														(φ)			
Flood plain (FP)	S1	0	33.3	63.5	3.2	1.5	5.5	6.5	10	9.8	28.8	30.9	0.2	0.3	3.3	4.16	2.04	-0.16	1.45
	S2	0	20.3	76	3.7	0.3	1.6	1.6	2.8	14	54.8	13.3	2	2.1	3.8	4.63	1.38	0.34	2.67
	S3	0	47.5	51.3	1.2	0.4	4	9.3	20	13.8	21.7	18	5.2	5.1	1.3	4	1.9	0	0.97
	S4	0	25.4	73.8	0.8	0.6	2.3	3.8	9.3	9.4	39.5	32.8	0.3	0.3	0.9	4.39	1.31	-0.34	1.36
	S5	0	36.5	63.1	0.4	0.5	2.4	4.3	14.6	14.7	26.5	36	0.1	0.1	0.4	4.2	1.4	-0.26	0.9
	S6	0	55	43.6	1.4	1.1	5.4	10.5	21.3	16.7	22.2	19	0.5	0.5	1.4	3.66	1.64	-0.12	0.84
	S7	0	73	23.8	3.2	0.8	1.8	11.4	36.7	22.3	13.1	4.5	1.5	1.6	3.1	3.25	1.74	0.41	1.65
	S8	0	52.8	42.8	4.4	0.4	1.7	4.7	25.6	20.4	26.1	6.7	2.7	2.8	4.5	4.04	1.91	0.25	1.49
	S9	0	40.6	54.4	5	0.1	1.7	4.5	17.5	16.8	22.4	16.2	5.3	5.3	5.2	4.6	2.18	0.26	1.14
Dune field (DF)	S10	0	66.5	30.3	3.2	0.3	4.5	13.4	28.7	19.6	18.7	5.4	1.4	1.5	3.3	3.3	1.9	0.26	1.57
	S11	0	73	24	3	0.2	5.3	12.4	31.2	23.9	12.9	4.2	1.9	2	3	3.21	1.86	0.3	1.67
	S12	0	66.8	30.6	2.6	1.2	3.8	9	30.5	22.3	17.5	5.4	2.5	2.5	2.7	3.45	1.81	0.26	1.65
	S13	0	76.8	21.8	1.4	1.7	5.6	12.3	32.6	24.6	16.7	1.9	0.9	0.9	1.4	2.99	1.39	0.06	1.19
	S14	0	86.3	12.6	1.1	0.6	2.5	21.2	48.8	13.2	9.4	1.1	0.5	0.5	1.1	2.65	1.11	0.28	1.36
	S15	0	73	25.8	1.2	0.4	4.5	12	33	23.1	16.1	4.1	2.4	2.3	0.9	3.13	1.5	0.22	1.28
	S16	0	73.3	23.3	3.4	0.5	6.2	16.1	35.4	15.1	14.2	2.6	1.5	1.6	3.4	2.98	1.94	0.34	1.58
	S17	0	70.7	25.6	3.7	0.3	10.4	20.6	22.4	17	13.4	4.3	2	2	3.9	3.01	2.17	0.29	1.24
	S18	0	80.5	17.1	2.4	0.2	10.1	13.8	33.2	23.2	10.8	1.2	1.3	1.3	2.5	2.75	1.8	0.17	1.69
Distal part of alluvial fan (DA)	S19	1.1	37.7	56.1	6.2	1.1	2.4	4.5	16.6	13.1	31.5	10.8	3.7	3.7	6.4	4.63	2.32	0.25	1.31
	S20	9.2	55.8	41.4	2.8	2.9	8.5	10.6	19.3	14.5	26.7	8.5	1.6	1.7	2.9	3.4	2.15	-0.03	1.31
	S21	11.4	32.7	63.6	3.7	1.7	2.9	4.7	12.3	11.1	37.3	13.6	4.4	4.4	3.9	4.37	2.02	0.05	1.66
	S22	26.8	48.5	48.4	3.1	3.8	5.7	8.1	18.7	12.2	34.5	6.9	1.9	1.9	3.2	3.64	2.08	-0.02	1.44
	S23	28	51.1	46.4	2.5	4.9	6.2	7.1	18.2	14.7	33.4	7.7	1.3	1.4	2.6	3.53	2.05	-0.18	1.48
	S24	32.2	72.9	25.6	1.5	7.9	9.5	13	28.2	14.3	18	3.9	1	1.1	1.6	2.67	1.9	0.03	1.07
	S25	40	51.6	44.6	3.8	8.1	9.6	8.6	14.2	11.1	28.4	8.8	1.7	1.8	3.9	3.38	2.52	-0.13	1.24
	S26	24.2	39.1	56.3	4.6	3.7	6.4	8.1	11.8	9.1	32.9	13.5	2.5	2.6	4.8	3.96	2.37	-0.12	1.33
	S27	43.6	28.3	65.8	5.9	5.3	5.3	4.2	6	7.5	32.7	18.7	4.1	4.2	6.1	4.62	2.6	-0.01	1.84
	S28	54.1	47.7	47.4	4.9	8.7	9.1	8.6	11.7	9.6	27.7	10.2	2.2	2.3	5	3.57	2.68	-0.13	1.21
	S29	71.3	73.2	24.6	2.2	25.1	20.4	12.5	10.1	5.1	13.1	6.3	1.5	1.5	2.2	1.92	2.56	0.44	0.83
	S30	71.4	39.2	56.9	3.9	7.9	8.2	6.3	8.9	7.9	33.9	13.3	2.8	2.8	4.1	3.7	2.58	-0.21	1.31
Max		71.4	86.3	76	6.2	25.1	20.4	21.2	48.8	24.6	54.8	36	5.3	5.3	6.4	4.63	2.68	0.44	2.67
Min		0.0	20.4	12.7	0.4	0.1	1.6	1.6	2.9	5.1	9.4	1.1	0.1	0.1	0.4	1.92	1.11	-0.34	0.83
Sd		21.81	20.42	19.08	1.48	4.88	3.82	4.71	11.24	5.29	10.98	9.16	1.35	1.33	1.52	0.73	0.41	0.40	0.35

MS: Medium sand, FS: Fine sand, VFS: Very fine sand, VCSi: Very coarse silt, CSi: Coarse silt, MSi: Medium silt, FSi: Fine silt, VFSi: Very fine silt, Mz: Mean grain size, δI: Sorting, SKI: Skewness, K: Kurtosis

Table 2. Summary of particle size distribution stattisticd in the geomorphic surfaces and total area

Geomorphic surface	Sample code	Gravel	Sand	Silt	Clay	VCS	CS	MS	FS	VFS	VCSi	CSi	MSi	FSi	VFSi	Mz	□I	SKI	K
		%														(φ)			
Flood plain (FP)	Max	0	20.3	23.8	0.4	0.1	1.6	1.6	2.8	9.4	13.1	4.5	0.1	0.1	0.4	3.25	1.31	-0.34	0.84
	Min	0	73.0	76.0	5.0	1.5	5.5	11.4	36.7	22.3	54.8	36	5.3	5.3	5.2	4.63	2.18	0.41	2.67
	Mean	0	42.7	54.7	2.6	0.6	2.9	6.3	17.5	15.3	28.3	19.7	2.0	2.0	2.7	4.10	1.72	0.04	1.39
	SD	0	16.3	16.6	1.7	0.4	1.6	3.4	10	4.3	12.2	11.3	2.1	2.0	1.7	0.44	0.31	0.28	0.56
Dune field (DF)	Max	0	66.5	12.6	1.1	0.2	2.5	9.0	22.4	13.2	9.4	1.1	0.5	0.5	0.9	2.65	1.11	0.06	1.19
	Min	0	86.3	30.6	3.7	1.7	10.4	21.2	48.8	24.6	18.7	5.4	2.5	2.5	3.9	3.45	2.17	0.34	1.69
	Mean	0	74.1	23.5	2.4	0.6	5.9	14.5	32.9	20.2	14.4	3.4	1.6	1.6	2.5	3.05	1.72	0.24	1.47
	SD	0	6.4	5.8	1.0	0.5	2.7	4.1	7.0	4.2	3.1	1.7	0.7	0.7	1.1	0.25	0.33	0.08	0.20
Distal part of alluvial fan (DA)	Max	1.1	28.3	24.6	1.5	1.1	2.4	4.2	6.0	5.1	13.1	3.9	1.0	1.1	1.6	1.92	1.90	-0.21	0.83
	Min	71.4	73.2	65.8	6.2	25.1	20.4	13.0	28.2	14.7	37.3	18.7	4.4	4.4	6.4	4.63	2.68	0.44	1.84
	Mean	34.4	48.2	48.1	3.8	6.8	7.9	8.0	14.7	10.9	29.2	10.2	2.4	2.5	3.9	3.62	2.32	-0.01	1.34
	SD	22.8	14.2	13.1	1.4	6.3	4.6	2.9	5.9	3.1	7.1	4.1	1.1	1.1	1.5	0.78	0.27	0.19	0.26
Total area	Max	71.4	86.3	76	6.2	25.1	20.4	21.2	48.8	24.6	54.8	36.0	5.3	5.3	6.4	4.63	2.68	0.44	2.67
	Min	0	20.4	12.7	0.4	0.1	1.6	1.6	2.9	5.1	9.4	1.1	0.1	0.1	0.4	1.92	1.11	-0.34	0.83
	Mean	13.8	54.3	42.7	3.0	3.1	5.8	9.5	21.0	15	24.5	11.0	2.0	2.1	3.1	3.59	1.96	0.08	1.39
	SD	22.2	18.4	17.9	1.5	5.0	3.9	4.8	10.9	5.4	10.4	9.2	1.4	1.4	1.6	0.69	0.42	0.22	0.36

MS: Medium sand, FS: Fine sand, VFS: Very fine sand, VCSi: Very coarse silt, CSi: Coarse silt, MSi: Medium silt, FSi: Fine silt, VFSi: Very fine silt, Mz: Mean grain size, δI: Sorting, SKI: Skewness, K: Kurtosis

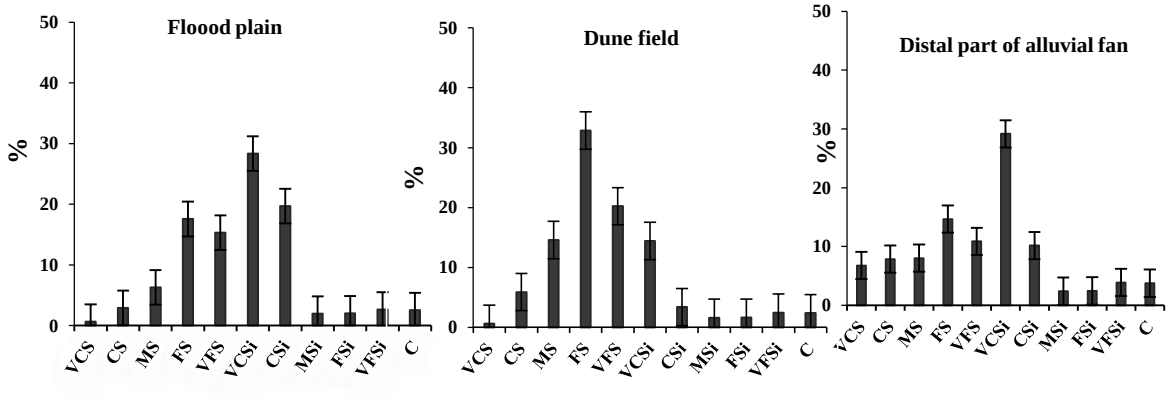

Figure 2. Average particle size distribution of the surface sediments in studied geomprphic surfaces; VCS: very coarse sand, CS: coarse sand, MS medium sand, FS fine sand, VFS very fine sand, VCSi, very coarse silt, CSi coarse silt, MSi medium silt, FSi fine silt, VFSi very fine silt, C clay

Particle size distribution can, to some extent, reveal the type of sedimentary environment and the processes that influence particle transport. Each sedimentary environment tends to produce a characteristic shape of frequency curve. Figure 3 presents the frequency curves of particle size distribution (based on the phi scale) for the three geomorphic surfaces. The floodplain (FP) surface exhibited a bimodal distribution, with the first mode at 2.5 phi (fine sand) and the second at 4.5 phi (very coarse silt). This suggests multiple sediment sources. The distal alluvial fan (DA) surface showed a similar bimodal pattern, also with modes at 2.5 and 4.5 phi. In contrast, the dune field (DF) surface displayed a unimodal distribution, with a single mode at 2.5 phi in the fine sand range.

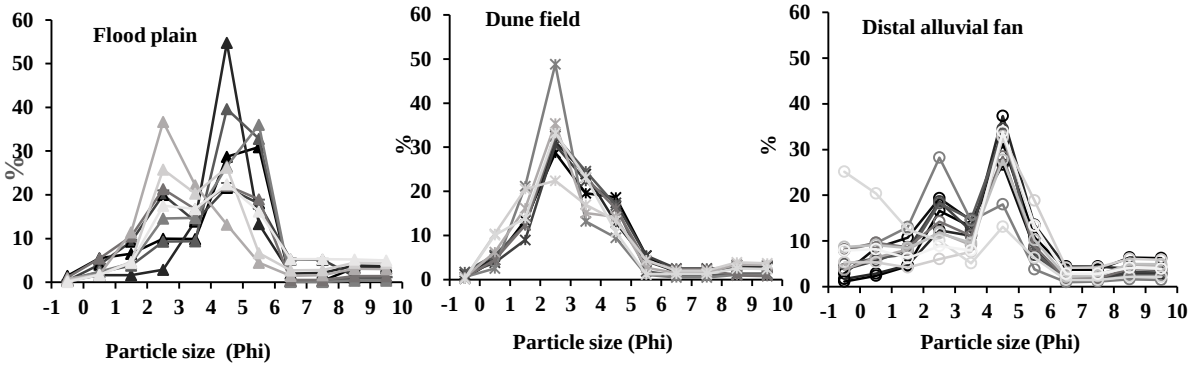

Figure 3. Frequency distribution curves of grain size in the studied geomorphic surface

As illustrated in Figures 2 and 3, particles on the DA and FP surfaces are predominantly fine sand and very coarse silt. Compared to the DF surface, both DA and FP show reduced sand content and increased silt content. These results suggest that different sedimentary processes are responsible for the bimodal grain-size distributions observed on the FP and DA surfaces. While, the aeolian sediments of the DF surface are primarily unimodal.

3.2. Statistical parameters of particle size distribution

On the FP surface, Mz ranged from 3.25 to 4.63 phi (average 4.10 phi); on the DF surface, from 2.65 to 3.45 phi (average 3.05 phi); and on the DA surface, from 1.92 to 4.63 phi (average 3.62 phi) (Tables 1 and 2). In many sand seas around the world, the average particle diameter typically is between 1.60 and 2.65 phi (Lancaster, 1995; Dong et al., 2011). The reported values for Mz are 2.43 phi in the Kumtagh Desert (Dong et al., 2011), 2.26 phi in the sandy dunes of the Ejina Desert (Zhou et al., 2011), 2.56 phi in the barchan dunes of the Tengger Desert (Zhang et al., 2015), and 2.37 phi in the eastern deserts of China (Zhang et al., 2015). In the Hexi Desert, Zhang and Dong (2015) found that aeolian sediments consisted mainly of fine and very fine sand. In the Badain Jaran Desert, sediments were dominated by fine and medium sand, with mean grain sizes ranging from 2.1 to 2.7 phi (Dong et al., 2013). Compared to these typical sand seas (Lancaster, 1995), the Mz values on the FP and DA surfaces in our study area are finer. This difference reflects the lower sand content in our samples relative to the >95% sand content in pure sand seas. Whereas, the sand content from the DF surface falls well within the expected range for global aeolian sand dunes.

Transport processes play a key role in shaping particle size distribution and, influence sedimentological parameters. In this study, the FP and DA surfaces exhibited higher Mz values than the DF surface, indicating that particles on the DF surface are coarser. Compared with other desert environments worldwide, the geomorphic surfaces in our study area contain finer particles. The higher Mz values observed on the FP surface can be attributed to the presence and seasonal flooding of the Kal-e Shur River. On the DA surface, the higher Mz values are likely due to streamflow originating from the southern highlands of the study area.

The particle size distributions observed in this study align with findings from other aeolian systems in Iran. Ghazi et al. (2019) reported average Mz values of 2.66 phi for aeolian-dominated sands in southwestern Iran, which are slightly coarser than those on our DF surface (average 3.05 phi). In contrast, their fluvially influenced samples exhibited bimodal distributions comparable to our FP and DA surfaces. Mohammadi (2023) documented an eastward transition from aeolian processes (sand dunes) to fluvial or alluvial processes (distal alluvial fans) in the Makran coastal plains. The Mz of our DF surface is finer than the aeolian-dominated sands reported by Mohammadi (2023) on the western Makran coast. This difference is likely attributable to variations in source material proximity and local wind regimes.

As shown in Table 2, the sorting on the FP surface ranged from 1.31 to 2.18 phi (average 1.72 phi); on the DF surface, from 1.11 to 2.17 phi (average 1.72 phi); and on the DA surface, from 1.90 to 2.68 phi (average 2.32 phi). These values indicate that the sediments are poorly to very poorly sorted. Sorting was slightly better on the DF surface than on the FP, while the DA surface exhibited the poorest sorting. The simultaneous influence of fluvial and aeolian processes on the FP and DA surfaces likely explains these results. The interaction of these two transport mechanisms mixes sediments of different grain sizes, leading to wider grain-size distributions and consequently poorer sorting. In contrast to the well-sorted, aeolian-dominated barchan dunes of the Tabas Erg in central Iran (Ghayeni et al., 2025), the sandy sediments of southern Sabzevar are poorly sorted and display mixed aeolian-fluvial characteristics. This distinction reflects their transitional geomorphic setting along the margin of the Great Kavir. Zhang et al. (2018) reported average particle sorting in the eastern desert regions of China as 0.78 phi (range: 0.57–0.78), indicative of poor to very poor sorting. This represents weaker sorting compared to the Taklamakan sand sea (0.39 phi; Zhou, 2007) and the Badain Jaran Desert (0.49 phi; Kian et al., 2011).

Skewness on the FP, ranged from -0.34 to 0.41 (mean 0.04); on the DF, from 0.06 to 0.34 (mean 0.24); and on the DA, from -0.21 to 0.44 (mean -0.01). The most negative skewness

occurred on the FP surface, indicating a tendency toward coarser particles, a signature of fluvial activity associated with the Kal-e Shur River. The most positive skewness was observed on the DA surface, suggesting a finer particle bias that reflects fluvial input from the southern highlands and the transport of fine-grained material. Kurtosis (K) values showed the following ranges. On the FP, from 0.84 to 2.67 (mean 1.39); on the DF, from 1.19 to 1.69 (mean 1.47); and on the DA, from 0.83 to 1.84 (mean 1.34).

3.3. Bivariate plots parameters of particle size distribution

Bivariate plots illustrate the relationship between two particle size distribution parameters and are useful for interpreting transport and depositional processes (Zhou and Yu, 2014; Zhang and Dong, 2015; Karimi et al., 2017). On the DF surface, a clear relationship found between δI and Mz, as Mz increases sorting becomes poorer. However, on the FP and DA surfaces, no significant change in sorting is observed with increasing Mz (Figure 4).

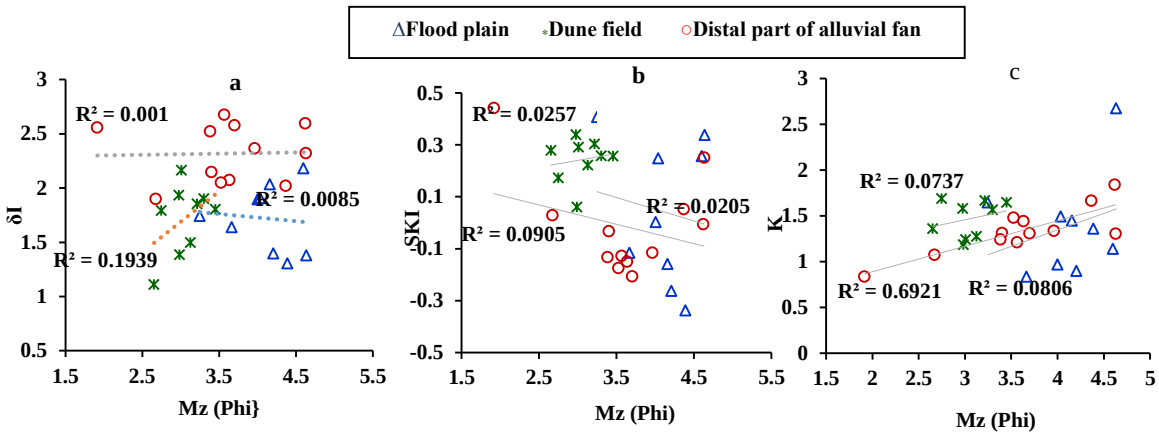

Figure 4. Bivariate plots of mean Mz (mean grain size) with sorting (δI), skewness (SKI), and kurtosis (K) in the studied geomorphic surfaces

In many studies of aeolian sandy sediments, where wind is the only factor affecting particle size distribution, a systematic relationship is typically observed between Mz and other grain-size parameters (Zhou and Yu, 2014; Zhang and Dong, 2015; Karimi et al., 2017). In the present study, however, a meaningful correlation between Mz and sorting was found only on the DF surface. The weak or absent correlation between Mz and sorting on the FP and DA surfaces (Figure 4) reflects the bimodal nature of sediments in these geomorphic settings. In systems where sediments originate from multiple sources (fluvial and aeolian) and have experienced different transport histories, the expected systematic relationship between Mz and sorting often breaks down. This occurs because the mixing of distinct sediment populations disrupts the sorting signature imparted by any single process (Zhang and Dong, 2015). The bimodal particle size distributions observed on the FP and DA surfaces (Figure 3) indicate the presence of two sediment populations of fine sand and very coarse silt. Their mixing produces poor sorting and a weak Mz‑sorting correlation. In contrast, the DF surface, which receives sediment primarily through aeolian processes, exhibits a clearer relationship between Mz and sorting (Figure 4), consistent with findings from other unimodal aeolian systems (Zhou and Yu, 2014). The absence of correlation on the FP and DA surfaces serves as a diagnostic signature of mixed aeolian‑fluvial processes. This interpretation is independently supported by the bimodal

frequency curves as well as by SEM microtextural evidence (Figures 6-8), which reveals both fluvial and aeolian features on quartz grains from these surfaces.

3.4. Analysis of surface microtexture of quartz grains

Quartz is the most abundant mineral in sedimentary environments. Due to its high resistance to physical and chemical weathering, the effects of transport processes are well preserved on its surface. Quartz surface textures provide valuable information for identifying transport mechanisms and sedimentary environments (Wass et al., 2014; Ma et al., 2024). For microtexture analysis, quartz grains were selected. To confirm that the particles examined were indeed quartz, elemental analysis was performed using EDS (Figure 5).

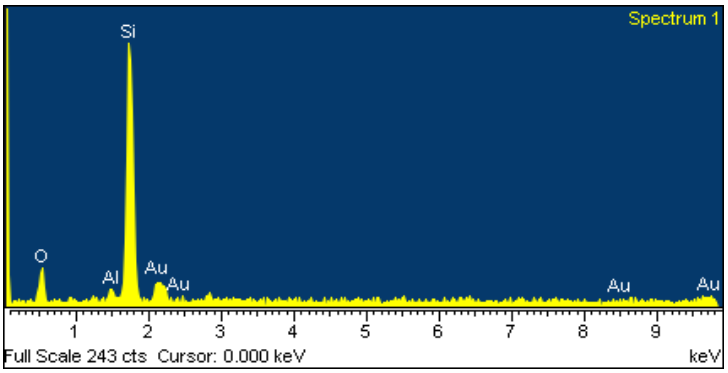

Figure 5. EDS spectrum of quartz grain of S20 sample from distal part of alluvial fan; the presence of only Si and O elements confirmed the occurrence of quartz

Figure 6 presents a scanning electron microscope (SEM) image of sample S3 from the FP surface. As shown in Figures 6a and b, the sediments consist of a mixture of angular and sub-rounded particles, with angular forms predominating. The main microtextures observed on quartz grains include low-relief V-shaped fractures, low-relief crescent gouges, deeply abraded V-shaped fractures, low-relief irregularities resulting from chemical dissolution, fractures with semi-sharp edges and V-shaped cavities, multiple V-shaped fractures, and percussion cracks infilled with fine particles along the edges (Figures 6c-d). Recent studies have shown that V-shaped features can form through various processes, including particle collision in both alluvial and aeolian environments, as well as chemical dissolution (Ma et al., 2024; Woronko et al., 2017; Mejía-Ledezma et al., 2020). Linear and stepped cavities and cracks on the surface texture of sand grains indicate particle collision during transport, specifically through saltation and creep driven by wind (Sweet, 2010).

In aqueous environments, grain-to-grain collision tends to produce V-shaped features, irregular pits, large fractures, dissolution features, and secondary crystal growth. Considering the abundance of angular grains on the FP surface, along with the presence of V-shaped features, deep but worn fractures, and percussion fractures on quartz grain surfaces, it can be concluded that the sediments have a dual origin. They were initially transported by high-energy processes and later modified by low-energy processes.The occurrence of irregularities from chemical dissolution and pits infilled with fine grains further points to a riverine influence on these sediments. The evidence suggests that the FP sediments have been affected by the Kal-e Shur River. Recent research indicates that the combination of surface features such as V-shaped fractures and dissolution-related irregularities can reflect the combined influence of chemical and mechanical processes (Ma et al., 2024; Woronko et al., 2017; Mejía-Ledezma et al., 2020).

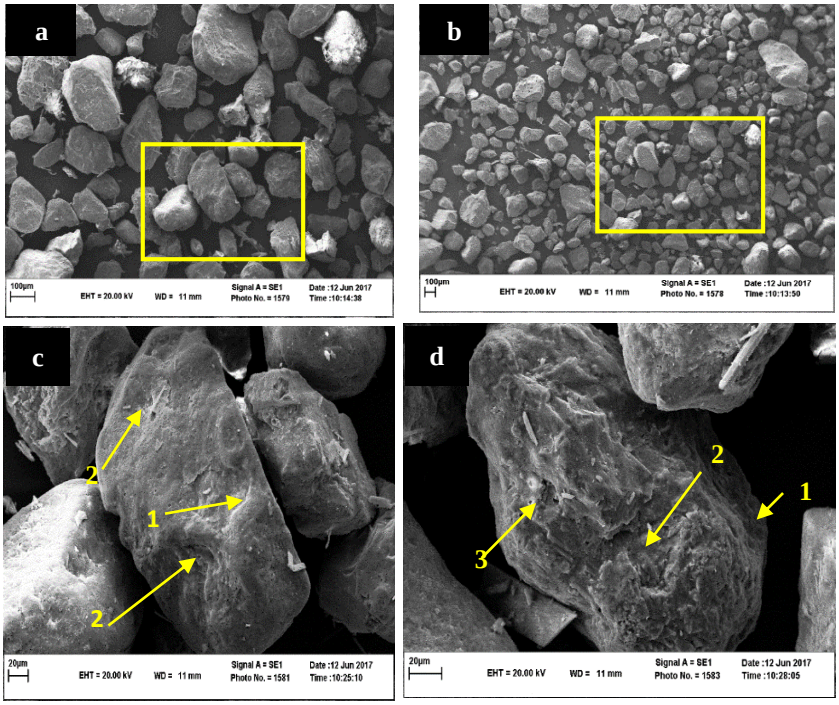

Figure 6. SEM micrographs of sand quartz grains in flood plain surface (FP); a and b) angular and sub-rounded grains, C) 1. low relief crescent gouges, 2. deep abraded fatigue d) 1. low-relief irregularities due to chemical dissolution, 2. curved and stepped fracture and cavities and 3 percussion pits filled with fine particles at the edges

Pourali et al. (2023) documented that surface sediments in the Sabzevar playa are predominantly aeolian, with quartz grains exhibiting rounded to sub-rounded morphologies, whereas deeper sediments retain angular features indicative of fluvial transport. This pattern mirrors our own observation that DF surface grains are sub-rounded to rounded compared to the angular grains on the DA surface. Furthermore, the microtextural features we observed—particularly V-shaped percussion marks and conchoidal fractures—have been shown by Bónová et al. (2021) in northeastern Iranian deposits to indicate multiple sedimentary cycles and combined aeolian–subaqueous transport histories.

Figure 7 presents SEM images of sample S17 from the DF surface. The grains are predominantly sub-rounded to rounded, with a small proportion of sub-angular forms (Figures 7a-b). Observed microtextures include parallel grooves with multiple fractures, crescentic fractures, conchoidal fractures, and craters (Figures 7c-d). The presence of sub-angular grains alongside incompletely rounded forms suggests that the grains have traveled only a short distance from their source. Conchoidal fractures and craters on grain surfaces indicate transport by creep and saltation, as well as grain-to-grain collision. Parallel grooves are interpreted as resulting from particle movement and dragging during aeolian processes (Mejía-Ledezma et al., 2020). These features indicate that the DF sediments accumulated under a dominant aeolian regime.

Figure 8 presents SEM images of sample S20 from the DA surface. As shown in Figure 8a, the particles consist of a mixture of coarse and fine grains, all of which are completely angular. The presence of deep cracks on grain surfaces (Figure 8b), regular and angular edges, percussion fractures, smooth surfaces with flaky fractures, and multiple V-shaped fractures (Figure 8d) indicates a high-energy sedimentary environment and deposition under hydraulic processes. Over time, the sediments gradually became sub-angular during transport. The

coexistence of fine and coarse grains suggests sediment disturbance by multiple agents, in this case, fluvial and aeolian transport processes operating together on the DA surface.

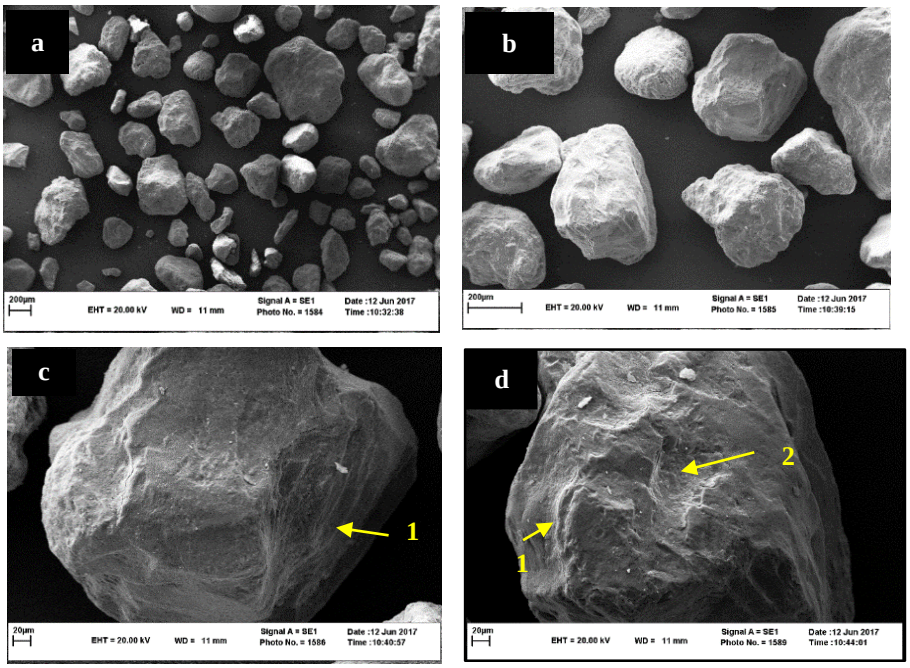

Figure 7. SEM micrographs of sand quartz grains in dune field surface (DF) surface; a and b) rounded to sub-rounded grains, c) 1. Parallel grooves, 2. conchoidal fracture and d) 1. crescentic depressions fracture, 2, crater

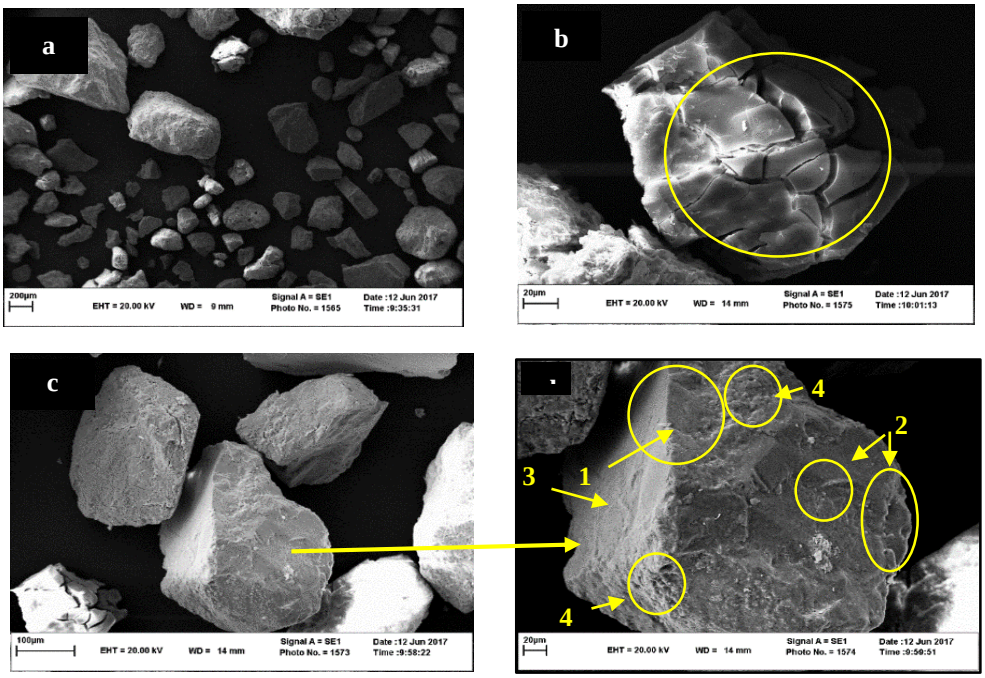

Figure 8. SEM micrographs of sand quartz grains in distal alluvial fan surface (DA) surface; a) mixture of coarse and fine angular to sub-rounded grains, b) deep cracks; c) sharped edges and flat cleavage surface; d) 1. regular and sharp edges, 2. percussion fractures, 3. smooth surfaces with flaky fractures and 4. multiple V-shaped fractures

4. Conclusion

This study investigated particle size distribution and quartz grain microtexture across three geomorphic surfaces (floodplain, dune field, distal alluvial fan) in the southern Sabzevar region, a transitional zone between the Alborz Mountains and the Great Kavir desert. The key findings are: (1) bimodal particle size distributions (fine sand + very coarse silt) in FP and DA indicate mixed aeolian-fluvial sources; (2) unimodal distributions (fine sand only) in DF indicate aeolian dominance; and (3) SEM microtextures-V-shaped fractures and conchoidal features in DF versus angular grains and dissolution pits in FP/DA-independently confirm these process interpretations. The methodological implication is that bimodality in particle size distribution, combined with quartz microtexture analysis, provides a robust tool for discriminating aeolian-fluvial interactions in other unstudied arid basins. The Sabzevar region, with its juxtaposed geomorphic surfaces, demonstrates how sedimentological proxies can distinguish process regimes even when sources are geographically close and lithologically similar.

Comparison with other Iranian basins reveals that Sabzevar occupies an intermediate position between purely aeolian ergs and fluvially-dominated playa systems. The mixed signatures in FP and DA resemble documented mixed-process basins elsewhere on the Iranian plateau, while the DF surface shares characteristics with more purely aeolian systems. We recommend using geochemical and mineralogical proxies to better characterize the sediments and identify their provenance.

Acknowledgment

We are grateful to Ferdowsi University of Mashhad Research for financial support of this study.

Author Contributions

The authors contributed to the study conception and design. AK and FJ, prepared the samples and performed the experiments. FJ analysed the samples in the laboratory. FJ write the first draft of the manuscript with support of AK. AK and FJ finalized the manuscript.

Funding

This study supported by a grant from Ferdowsi University of Mashhad, Iran (Grant number: 3/55426; 1400/05/12).

Competing interests

The authors have no conflicts of interest to declare that are relevant to the content of this article.

Data availability

The data are available from on request.

References

Abouda, J. A. Z. (2003). Grain size distribution and composition of modern dune and beach sediments, Malindi Bay coast, Kenya. *Journal of African Earth Sciences*, 36, 41-54. https://doi.org/10.1016/S0899-5362(03)00016-9

Blott, S. J., & Pye, K. (2001). GRADISTAT: a grain size distribution and statistics package for the analysis of unconsolidated sediments. *Earth Surface Processes and Landforms*, 26(11), 1237-1248. https://doi.org/10.1002/esp.261

Bónová, K., Jafarzadeh, M., & Bóna, J. (2021). Depositional history of the Devonian Ilanqareh and Padeha formations in Azarbaijan Province and Eastern Alborz (Iran): constraints from heavy-mineral microtextures. *Acta Geologica Slovaca*, 13(1), 13-26.

Burt, R. (2004). Soil survey laboratory methods manual. Soil Survey Investigations Report No. 42. Version 4.0., USDA-NRCS, Lincoln, Nebraska.

Dong, Z. B., Qu, J. J., Qian, G. Q., & Zhang, Z. C. (2011). Aeolian geomorphological zonation of the Kumtagh Desert. *Journal of Desert Research*, 4, 002.

Dong, Z., Quan, G., Lv, P., & Hu, G. (2013). An overview of the sand sea with the tallest dunes on earth: The Badain Jaran sand sea of China. *Earth-Science Reviews*, 120, 20-39. https://doi.org/10.1016/j.earscirev.2013.02.003

Folk, R. L., & Ward, W. C. (1957). Brazos River bar: a study in the significance of grain size parameters. *Journal of Sedimentary Research*, 27(1), 3-26. https://doi.org/10.1306/74D70646-2B21-11D7-8648000102C1865D

Ghayeni, H., Khanehbad, M., & Rashki, A. (2025). Grain size analysis and sedimentological characteristics of wind-blown sands: a case study of Barchan dunes in the Erg of Tabas, central Iran. *Aeolian Research*, 74, 100993.

Ghazi, A., Karimi, A., Haghnia, G. H., & Hojati, S. (2019). Grain size and mineralogical studies of sandy sediments in southwestern Iran. *Desert*, 24(1), 75-85. https://doi.org/10.22059/jdesert.2019.72442

Hamdan, M. A., Refaat, A. A., Anwar, E. A., & Shallaly, N. A. (2015). Source of the aeolian dune sand of Toshka area, southeastern Western Desert, Egypt. *Aeolian Research*, 17, 275-289. https://doi.org/10.1016/j.aeolia.2014.08.005.

Huang, J., Yu, H., Guan, X., Wang, G., & Guo, R. (2015). Accelerated dryland expansion under climate change. *Nature Climate Change*, 6(2), 166-171. https://doi.org/10.1038/nclimate2837

Ma, Y., Li, Z., Tan, D., Zou, X., & Tao, T. (2024). Grain size and surface micro-texture characteristics and their paleoenvironmental significance of Holocene sediment in southern margin of the Gurbantunggut Desert, China. J*ournal of Arid Land*, 16, 632-653. https://doi.org/10.1007/s40333-024-0015-1

Maghsoudi, M., & Ganjaeian, H. (2025a). Aeolian geomorphology of ergs and dunefields in Iran. *Desert*, 30(1), 42-66. https://doi.org/10.22059/jdesert.2025.102461

Maghsoudi, M., & Ganjaeian, H. (2025b). Classification of ergs around the Kavir plain (Dasht-e Kavir) and the Masileh playa and assessment of their changes. *Quaternary Journal of Iran*, 10(1), 88-107. (In Persian). https://doi.org/10.22034/irqua.2025.2054847.1042

Mejía-Ledezma, R. O., Kasper-Zubillaga, J. J., Álvarez-Sánchez, L. F., Mendieta-Lora, M., Arellano-Torres, E., Tetlalmatzi-Martínez, J. L., González-Bermúdez, A., Patiño-Andrade, D., & Armstrong-Altrin, J. S. (2020). Surface textures of quartz and ilmenite grains from dune and beach sands of the Gulf of Mexico Coast, Mexico: Implications for fluvial, aeolian and marine transport. *Aeolian Research*, 45, 100611. https://doi.org/10.1016/j.aeolia.2020.100611

Mohammadi, A. (2023). Aeolian and fluvial processes influence on dust storms of Hormuz Strait and Makran coastal plains (SE Iran); insight from geomorphic landforms, and sediment texture and mineralogy. *International Journal of Earth Sciences*, 112(7), 1973-1987. https://doi.org/10.1007/s00531-023-02335-0

Pourali, M., Sepehr, A., Hosseini, Z., & Hamzeh, M. A. (2023). Sedimentology, geochemistry, and geomorphology of a dry-lake playa, NE Iran: implications for paleoenvironment. *Carbonates and Evaporites*, 38: 9. https://doi.org/10.1007/s13146-022-00829-7

Rao, W., Chen, J. U. N., Yang, J., Ji, J., Li, G., & Tan, H. (2008). Sr-Nd isotopic characteristics of eolian deposits in the Erdos Desert and Chinese Loess Plateau: Implications for their provenances. *Geochemical Journal*, 42, 273-282. https://doi.org/10.2343/geochemj.42.273

Sweet, D. E., & Soreghan, G. S. (2010). Application of quartz sand microtextural analysis to infer cold-climate weathering for the equatorial Fountain Formation (Pennsylvanian–Permian, Colorado, USA). *Journal of Sedimentary Research*, 80, 666-677. https://doi.org/10.2110/jsr.2010.061

Tsoar, H., Levin, N., Porat, N., Maia, L. P., Herrmann, H. J., Tatumi, S. H., & Claudino, S. V. (2009). The effect of climate change on the mobility and stability of coastal sand dunes in Ceará State, NE Brazil. *Quaternary Research*, 71(2), 217-226. https://doi.org/10.1016/j.yqres.2008.12.001

Vos, K., Vandenberghe, N., & Elsen, J. (2014). Surface textural analysis of quartz grains by scanning electron microscopy (SEM): From sample preparation to environmental interpretation. *Earth-Science Reviews*, 128, 93-106. https://doi.org/10.1016/j.earscirev.2013.10.013

Wang, X., Dong, Z., Zhang, J., Qu, J., & Zhao, A. (2003). Grain size characteristics of dune sands in the central Taklimakan Sand Sea. *Sedimentary Geology*, 161, 1-14. https://doi.org/10.1016/S0037-0738(02)00380-9

Woronko, B., Dłużewski, M., & Woronko, D. (2017). Sand-grain micromorphology used as a sediment-source indicator for Kharga Depression dunes (Western Desert, S Egypt). *Aeolian Research*, 29, 42-54. https://doi.org/10.1016/j.aeolia.2017.10.001

Zandifar, S., Jamalian, A., & Naemi, M. (2024). Analyzing the sedimentological parameters and size distribution pattern in Hamoun Hirmand sediments. *Desert Management*, 12(1), 1-18. (In Persian). https://doi.org/10.22034/jdmal.2024.2024636.1456

Zhang, C., Shen, Y., Li, Q., Jia, W., Li, J., & Wang, X. (2018). Sediment grain–size characteristics of sediment particle size and correlations with the aeolian environment in the eastern desert region of China. *Science of the Total Environment*, 627, 586-599. https://doi.org/10.1016/j.scitotenv.2018.01.270

Zhang, Z., & Dong, Z. (2015). Grain size characteristics in the Hexi Corridor Desert. *Aeolian Research*, 18, 55-67. https://doi.org/ 10.1016/j.aeolia.2015.05.006

Zhang, Z., Dong, Z., & Li, J. (2015). Grain-size characteristics of dune networks in the Tengger Desert, China. *Geografiska Annaler: Series A, Physical Geography*, 97, 681-693. https://doi.org/10.1111/geoa.12108

Zhu, B. (2007). Geochemistry, hydrochemistry and sedimentology of the Taklamakan Desert in the Tarim Basin, northwestern China (Doctoral dissertation). Institute of Geology and Geophysics Chinese Academy of Sciences, Beijing, China.

Zhu, B. Q., Yu, J. J., Rioual, P., & Ren, X. Z. (2014). Particle size variation of aeolian dune depsoits in the lower reaches of the Heihe River, China. *Sedimentary Geology*, 301, 54-69. https://doi.org/10.1016/j.sedgeo.2013.12.006

Zhu, B., & Yu, J. (2014). Aeolian sorting processes in the Ejina desert basin (China) and their response to the sedimentary environment. *Aeolian Research,* 12, 111-120. https://doi.org/10.1016/j.aeolia.2013.12.004